Study of supercooled water droplet chain evolving in a cold environment: Experimental and modelling study

Stiti Mehdi[1], Labergue Alexandre*[1], Castanet Guillaume[1], Lemoine Fabrice[1]
[1]Loraine Université, CNRS, LEMTA, F-5400 Nancy, France
*Corresponding author: alexandre.labergue@univ-lorraine.fr

Abstract
Knowledge of the temperature of supercooled water droplet is essential for aircraft certification. In the present paper, characterisation of supercooled droplets is made by Laser Induced Fluorescence (LIF). LIF technique allows a discrimination of the state of the droplet and a measurement of the droplets temperature. The technique is here used to characterise droplets falling in a cold environment. An experimental setup designed for supercooled droplet generation is built allowing a control of the ambient temperature for minimum temperature of $-55°C$. The study is performed on a line of equally-spaced droplets. This configuration allows changing several parameters as the droplet diameter D_{inj} the inter-droplet distance and the droplet injection temperature T_{inj}. Heat transfers in a droplet line are well known in the literature and their effect on Sherwood and Nusselt are still an opened issue. In this study, Nusselt and Sherwood numbers are estimated from experimental results and compared with correlation of isolated droplets. The comparison allows a quantification of the droplet interaction effect on heat and mass transfers. It is then shown that the inter-droplet distance parameter has a strong influence on the evolution of the correction of both Nusselt and Sherwood numbers.

Keywords
Supercooled water, Temperature measurement, interacting droplet, Laser Induced Fluorescence

Introduction
Water can be found liquid for temperature lower than $-40°C$ in the atmosphere [1]. Supercooled droplets could impact aircraft surfaces and freeze instantaneously and may lead to severe hazards [2] as reduction of visibility, blockage of pitot tubes or reduction of flight performances. Tests in icing wind tunnel (IWT) are made by airframers in order to certified aircraft in icing conditions. In order to generate Supercooled Large Droplet (SLD), *i.e.* droplets having diameter larger than 50µm, new IWT have been developed. Due to the large droplet diameters, it is impossible to make the hypothesis that droplets are at the equilibrium with the air ambient temperature. Temperature, local hygrometry and droplets composition (*i.e.* solid or liquid) need to be measured in order to guarantee the icing condition of the IWT.
Currently, very few non-intrusive optical methods have the ability to characterise supercooled droplets. The Global Rainbow Thermometry (GRT) is a technique based on the measurement of the refractive index of a liquid [3]. The temperature dependence of the refractive index allows an absolute measurement of droplets temperature. Ambiguity on the water temperature measurement can be observed due to the parabola's forms of the refractive index as a function of the temperature [3]. In some cases, the knowledge of the air ambient temperature allows avoiding this ambiguity. Another group for droplet temperature measurements are based on the laser-induced fluorescence (LIF) and used a thermal dependency of a dye previously seeded in the liquid of interest. Ratiometric methods allow eliminating the dependence of parameters usually difficult to determine properly. It consists in measuring a ratio of the fluorescence signal intensity collected simultaneously on two different spectral bands having different thermal sensitivities. This technique is referred to two-colour laser-induced-fluorescence (2cLIF) and was mainly used in the case of droplets in strong evaporation [4], [5] or in combustion, and in the case of droplet impinging onto heated walls in the Leidenfrost regime [6], [7].
In the present paper, the 2cLIF is extended for supercooled droplets. In a previous paper, it has been shown that the use of a second ratio allows discriminate liquid droplets to solid one [8] [9]. It leads to the three-color two dyes LIF (3c2dLIF). Here, temperature measurements are performed on a line of supercooled equally-spaced droplets and flowing along a cold vertical chamber. Experimental results are then compared with numerical simulations that take into account the interaction of droplets on the heat and mass transfers.

Principle of two-color laser-induced fluorescence thermometry
The principle consists in dissolving an organic fluorescent dye at very low concentration in water. A laser excitation, tuned on the absorption spectrum of the dye molecule, is applied and the resulting fluorescence signal is measured. The use of temperature sensitive fluorescent dyes makes then droplet thermometry possible. The

fluorescent signal I_{fi} collected on a given spectral band i in a collection volume V_c, at a temperature T can be written as [10]:

$$I_{fi}(T) = K_i.V_c.I_0.c.e^{s_i.T}$$

(1)

with I_0 the local laser excitation intensity, c the fluorescent dye concentration, K_i a constant depending on both the dye and the optical chain detection and s_i the sensitivity in temperature of the dyes (s in $\%/°C$) on the spectral band i. Both parameters I_0 and V_c remain usually difficult to determine. They can be removed by collecting simultaneously the fluorescent signal on two spectral band I_{f1} and I_{f2}, having different temperature sensitivities, in order to derive a ratio R_{12}. For methods with two dyes seeded in the fluid (2c2d LIF), the ratio can be expressed as:

$$R_{12} = \frac{I_{f1}}{I_{f2}} = \frac{K_1 c_1}{K_2 c_2}.e^{(s_1-s_2)T}$$

(2)

Finally, a reference R_{120} at a known temperature (T_0) is required to eliminate both K_i and c_i. Therefore, a normalized ratio is obtained :

$$\frac{R_{12}}{R_{120}} = e^{(s_1-s_2)(T-T_0)}$$

(3)

where $s_1 - s_2$ denotes the temperature sensitivity of the normalized fluorescence ratio depending on both the dyes and the spectral band of detection and may be determined by a temperature calibration step.

Temperature measurement by 3c2d LIF for supercooled droplet's characterisation

Several tests on a single dye solution oriented our work toward a solution with two dyes seeded in the water. The selected solution consists of a mixture of Rhodamine 560 ($c_{rh560} = 0.5 * 10^{-5}\ mol.L^{-1}$) and Kiton Red ($c_{KR} = 0.5 * 10^{-6}\ mol.L^{-1}$). Indeed, these dyes have opposite temperature dependencies (Figure 1). The spectral band used for this study are:

$$band1 = [496 - 517]nm\ ;\ band2 = [595 - 615]nm\ and\ band3 = [540 - 560]nm.$$
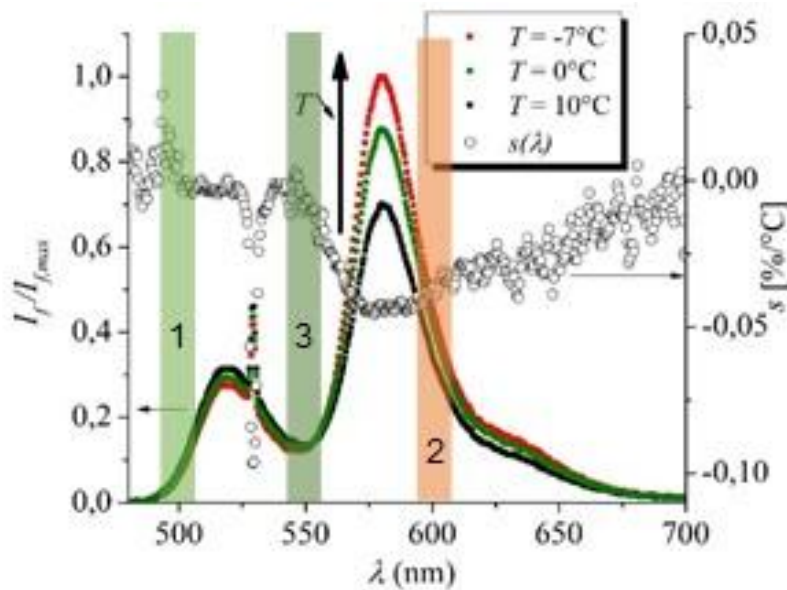

Figure 1. Typical spectra of the Kr/Rh560 mixture (left axis) for different temperatures normalized with the lowest temperature and evolution of the temperature sensitivity (right axis) as a function of the wavelength.

According the temperature calibration conducted in [10], the sensitivity $s_1 - s_2$ for the ratio R_{12} is 2.56%/°C.
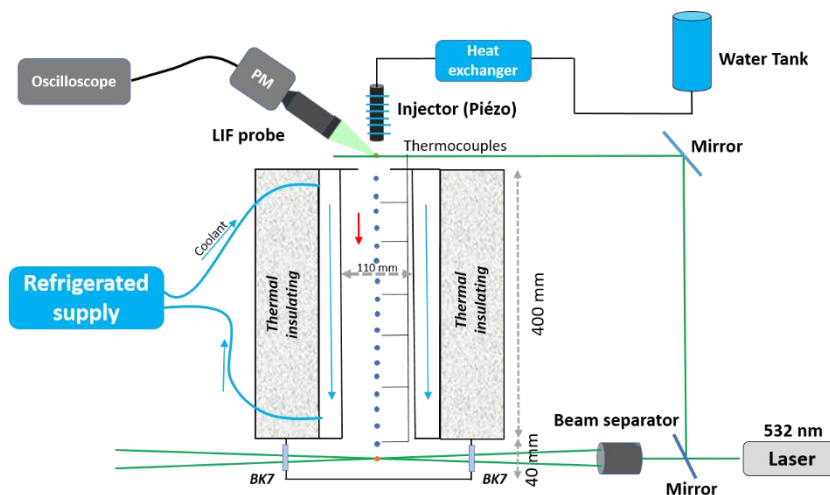
Figure 2. Experimental setup for the cooling of free fall droplet

Experimental setup

The set-up used to generate a line of equally-spaced supercooled droplets is presented in Figure 2. It is based on a double envelope cylinder [11], which is $400\ mm$ high and $110\ mm$ large in diameter. The top of the column is open permitting the droplets injection. Similarly, a test chamber with BK7 windows for optical measurements is implemented at the bottom of the columb. The internal air temperature is cool down by a means of a coolant flowing between both envelopes. The coolant temperature is controlled with the help of a cooler supply (Julabo Presto® system). The air temperature is measured by 6 thermocouples placed along the column. For a given temperature target of the cooled supply, a temperature difference appears between the top and the non-insulating test chamber of the column. Figure 3 gives the profile temperature along the column for two target temperatures ($-35°C$ and $-55°C$). The monodisperse droplets chain is generated by a piezoelectric droplet generator. The liquid jet coming out the injector is disintegrated into mono-sized droplets for specific vibrations frequencies of the piezoceramic attached to the injector body. The injector is water supplied by a pressurized water tank with air compressed between 0.15 and 6.5 bars. In order to obtain quickly supercooled droplets just after the injection, the droplets injection temperature T_{inj} is reduced close to 0°C by using a heat exchanger.
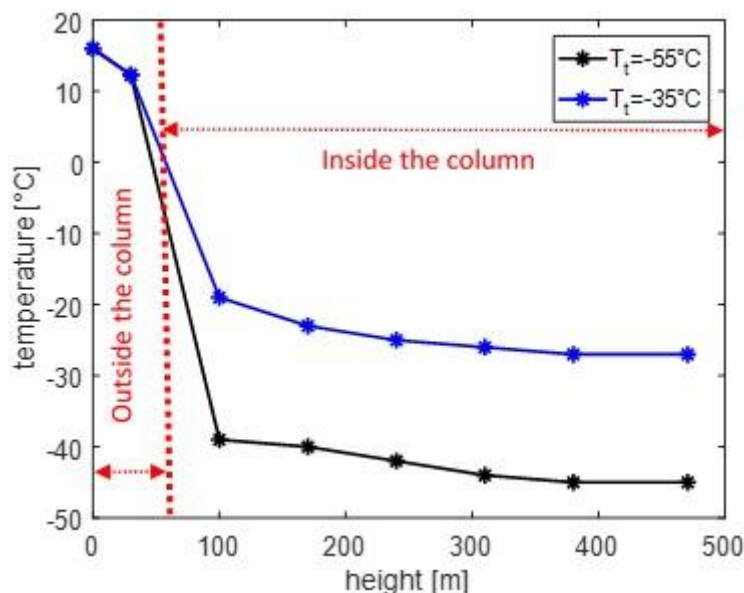

Figure 3. Example of a temperature profile inside the column

Measurements techniques

The fluorescence is induced by the green line of a continuous wave (CW) frequency-doubled Nd-YAG laser (beam wavelength of $\lambda = 532nm$; Ventus LaserQuantum®). The equally droplet spacing, as well as the droplet diameter at the injection, is controlled by using a second LIF measurement (fluorescence detected on the
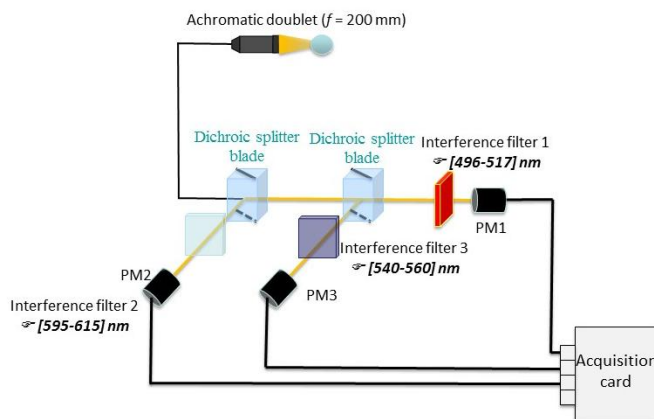

Figure 4. Detection LIF optical set-up

band $[590; 610]\ nm$) close to the injector exit (Figure 2).

The fluorescence signal is visualised with an oscilloscope and a perfect monodisperse chain is set by adjusting the frequency of the piezoelectric generator. Droplet temperature measurements are conducted at the test chamber corresponding to a distance of 475 mm from the droplet generator exit. The fluorescence signal is collected at right angle by means of an achromatic doublet (focal length of $200\ mm$) and coupled with an optical fibber having a core diameter of $70\ \mu m$. The fluorescence signal is then splited into both spectral bands by means of a dichroic and interference filters (Figure 4). The fluorescence is finally detected by two photomultiplier tubes and digitalized with an acquisition board. The accuracy of the technique is estimated on droplets close to the exit of the generator. Several acquisitions of $50\ 000$ droplets leads to an accuracy for the temperature of $\pm 0.8°C$. The droplet diameter D, the spacing parameter C (*i.e.* the ratio between the inter-droplet distance and the droplet diameter) and the droplet velocity V_{inj} at the injection are deduced from a metering flows. Additionally, Laser Doppler Velocimetry (LDV) measurements for droplet velocity was undergone (FlowLite® system; DantecDynamic manufacturer)(Figure 5).
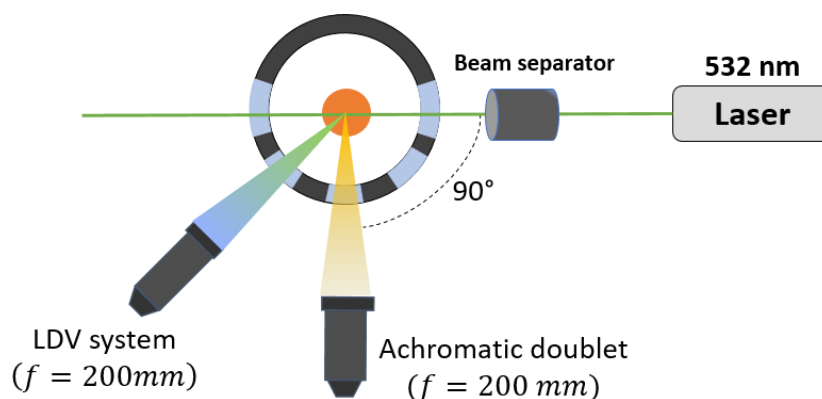

Figure 5. Top view of the column

Experimental results
All tested injection parameters are summarized in Table 1.

Target temperature	T_{inj} range [°C]	P_{inj} range [bar]	C range	V_{inj} range [m/s]	D_{inj} range [µm]	R_e range

$T_t = -55°C$	4.7-4.9	$0.2 - 0.5$	1.5-3.5	5.6-8.5	114-301	226-415
$T_t = -35°C$	4.9-0.1	$0.2 - 0.5$	1.7-5.6	4.3-8.6	76-271	160-370

Table 1. Injection conditions tested in the experiments

Measurements are performed for two different target temperatures. For each target temperature, the spacing parameter is changing by varying both the droplet generator frequency and the liquid injection pressure. Before to start each measurement, injection conditions are verified and measured: monodisperse character of the droplet chain, injection temperature and droplet diameter. It has to be noted that, due to the long height of the column, it was impossible to keep the monodisperse character of the droplet chain until the measurement point. Thus, it leads scattering results for LIF ratios. However, a physical dispersion of the measured temperature of $\pm 1°C$ was obtained due to the instability of the droplet chain as droplet coalescence or different values of droplets flying times. The experimental setup allows the measurement at a single point (*i.e.* at the bottom of the column). Therefore, a dimensionless time t^* is introduced in order to take account of the influence of the injection droplet diameter D_{inj} and the flying time t_{ft} .
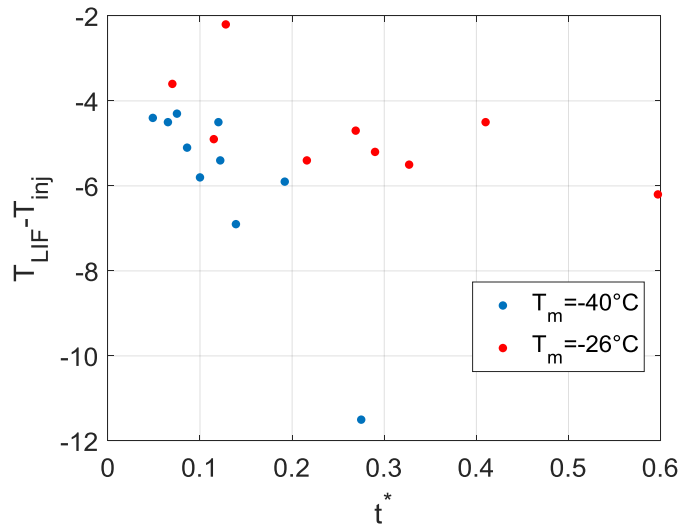

Figure 6. Cooling of the droplet in function of the dimensionless time t* for two different ambient temperature

$$t^* = \frac{a_l * t_{ft}}{D_{inj}^2}$$

Figure 6 depicts the droplets cooling defined as the local droplets temperature comparatively to the injection one as a function of the dimensionless time t^* for both target temperatures. When the target temperature is $-50°C$, a raise of the cooling of the droplets with t^* is observed. It shows that the cooling is intensified for smaller droplet and for droplet with having a long flying time in the cold environment.

Numerical Simulation

Comparison of the measurement with a model that takes into account the influence of the droplet interaction (Figure. 7) and the evaporation are undergone [5]. When a droplet falls in a cold environment, a part of the heat is used to evaporate the liquid and the other part is used to cool down the droplet. Both will result in a cooling of the droplet. The heat flux entering within the droplets depends on many things like the liquid/gas properties and the droplet spacing. Droplets interactions reduce the heat and mass transfers in comparison to the isolated droplets case (Figure. 8). Sh and Nu number are commonly used to characterise the heat and mass transfer between droplet and the gaseous environment. The heat flux ϕ_c received by the droplet can be expressed using the Nusselt number:

$$\phi_c = \pi.D.Nu.\lambda_g(T_{amb} - T_s)$$

T_S denoted the surface temperature of the droplet and λ_g the thermal conductivity of the gas. The mass flux of the vapour $\dot{m}$ due to the liquid evaporation can be expressed using the Sherwood number:

$$\dot{m} = \pi.D.\rho_g.D_\mu.Sh.B_M$$

With ρ_g the gas density, D_μ the diffusion coefficient of vapour in air. B_M is the mass transfer Spalding number related to the mass fraction of vapour at the drop surface and in the ambient gas. The expression of the $N_{u_{iso}}$ and Sh_{iso} number in the case of an isolated droplet were derived in a previous study [12].
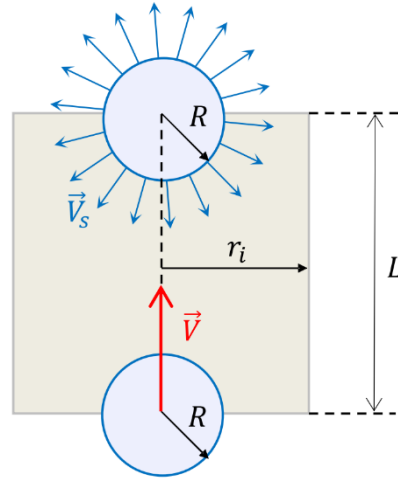
Figure 7. Region of influence of the droplet.

In the case of droplet interaction, reduction coefficients η_M and η_T are calculated according to:

$$\eta_M = \frac{Sh}{Sh_{iso}} \quad \eta_T = \frac{N_u}{N_{u_{iso}}}$$

Peclet and Schmidt number are almost equal and allow to made the hypothesis that $\eta_M = \eta_M = \eta$ leading to that the mass and thermal boundary layer are the same. Figure 8 presents a typical simulation result. Figure 8a describes the evolution of the relative droplet temperature (ie compared to the injection temperature) at the center Tc, the surface Ts and the mean value. Figure 8b gives the evolution of the droplet diameter divided by the droplet diameter at the injection. Figure 8b shows that the evaporation is very low. An effective model is used to
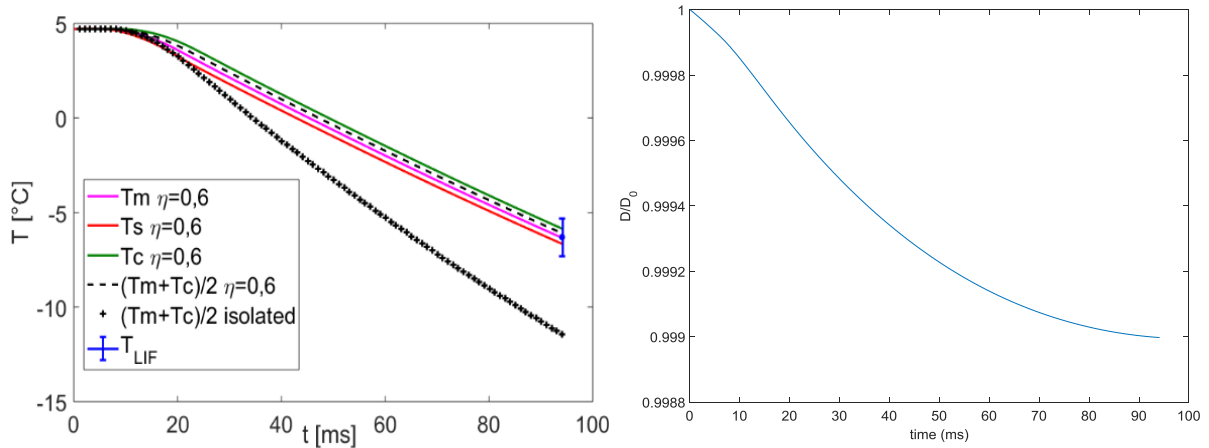

Figure 8. *A)* Comparison of the temperature measured by 3c2dLIF, the simulation with $\boldsymbol{\eta_m = \eta_t = 0.6}$ and the case of an isolated droplet. For a droplet with $\boldsymbol{T_{inj} = 4.7°C}$, $\boldsymbol{V_{inj} = 6.9\ m/s}$, $\boldsymbol{D_0 = 226\ \mu m}$ and $\boldsymbol{C_{inj} = 1.52}$. $\boldsymbol{T_m}$ is the mean temperature, $\boldsymbol{T_c}$ the center temperature, $\boldsymbol{T_S}$ the surface temperature and $\boldsymbol{T_{LIF}}$ the temperature measured by LIF *B)* Simulation of the droplets evaporation as a function of the time.

solve the heat equation and we observe that a thermic gradient exists within the droplet between the center T_c and the surface T_s. It has to be mentioned that the temperature measured by LIF technique is not exactly the volume-averaged temperature of the droplet. It has been shown [14] that LIF technique measure approximatively a temperature T_{LIF} equal to $T_{LIF} = \frac{T_m + T_c}{2}$ with T_m represents the mean temperature of the droplet. For each case, an optimisation of the reduction coefficients η is performed in order to fit our experimental data with simulation's result. For some points it has been observed that the droplet chain was not stable. The stability of the droplet chain was linked to the raise of the Re number. Indeed, for high Reynolds number turbulent flows around the droplets will destabilize the droplet chain. The destabilization of the droplet chain will render up to a raise of the heat transfer by a diminution of the droplets interaction. Figure 9 represents η as a function of the spacing parameter for different Re number. For a fixed Re number it can be observed that a small spacing parameter corresponds to a high reduction coefficient. We can observed that more the distance parameter is high more the temperature measured is close to the isolated droplet case. The comparison with experimental data from [5] for

$Re < 100$ are comparable and are in good agreement. However, for each Re range, it can be observed a raise of η with the spacing parameter.

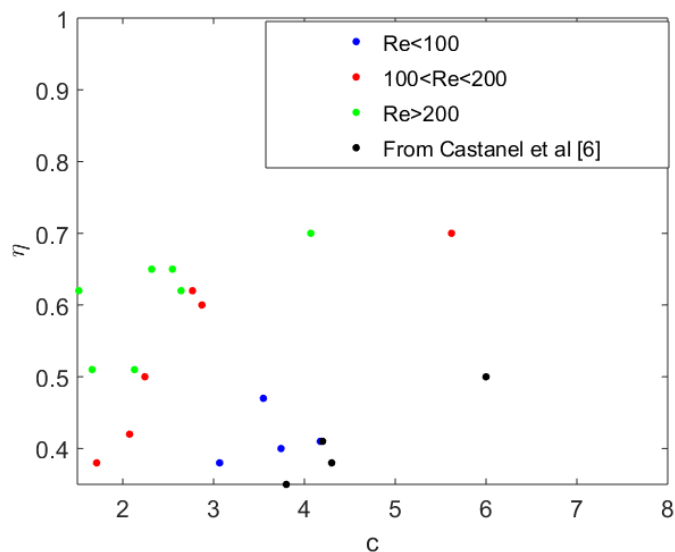**Figure 9**. η as a function of the spacing parameter for different Reynold number. Experimental data from [6] are added.

Conclusions

In this study, a ratiometric LIF technique using two dyes and three spectral bands of detection was used to characterize supercooled droplet. A sensitivity in temperature of $2.56\%/°C$ was obtained. Supercooled droplet chain was introduced in a chamber were the air ambient temperature may be cooled for minimum temperature of $-55°C$. The designated experimental setup allows the control and variation of a large number of parameter. Sherwood and Nusselt number are estimated from experiments and compared to the isolated droplet case in order to have information of the droplets interactions on the heat and mass transfer rates. The spacing parameter C appears to have a strong influence on the reduction of the Nusselt and Sherwood number. It has been shown that evaporation was very low and that for future works this parameter may be neglicted.

Acknowledgements

Nomenclature

a	Thermal diffusivity [s.m^{-2}]
c	Fluorescent dye concentration [mol. L^{-2}]
C	spacing parameter [-]
D	Droplet diameter [m]
If	Fluorescence signal intensity [-]
T	Temperature [°C]
t	Time [s]
V	Volume [m^3]
Sh	Sherwood Number [-]
Nu	Nusselt number [-]
Re	Reynold number [-]
λ	wavelength [m]
η	reduction coefficient [-]

References

[1] D. M. Murphy and T. Koop, 'Review of the vapour pressures of ice and supercooled water for atmospheric applications', *Q. J. R. Meteorol. Soc.*, vol. 131, no. 608, pp. 1539–1565, Apr. 2005.

[2] T. Cebeci and F. Kafyeke, 'Aircraft Icing', *Annu. Rev. Fluid Mech.*, vol. 35, no. 1, pp. 11–21, 2003.

[3] S. Saengkaew, G. Godard, and G. Grehan, 'Global Rainbow Technique: Temperature evolution measurements of super-cold droplets', ICLASS 2018, 2018.

[4]   L. Perrin, G. Castanet, and F. Lemoine, 'Characterization of the evaporation of interacting droplets using combined optical techniques', *Exp. Fluids*, vol. 56, no. 2, Feb. 2015.

[5]   G. Castanet, L. Perrin, O. Caballina, and F. Lemoine, 'Evaporation of closely-spaced interacting droplets arranged in a single row', *Int. J. Heat Mass Transf.*, vol. 93, pp. 788–802, Feb. 2016.

[6]   A. Labergue, J.-D. Pena-Carillo, M. Gradeck, and F. Lemoine, 'Combined three-color LIF-PDA measurements and infrared thermography applied to the study of the spray impingement on a heated surface above the Leidenfrost regime', *Int. J. Heat Mass Transf.*, vol. 104, pp. 1008–1021, 2017.

[7]   W. Chaze, O. Caballina, G. Castanet, and F. Lemoine, 'Spatially and temporally resolved measurements of the temperature inside droplets impinging on a hot solid surface', *Exp. Fluids*, vol. 58, no. 8, Aug. 2017.

[8]   M. Stiti, A. Labergue, D. Stemmelen, S. Leclerc, and F. Lemoine, 'Temperature measurement and state determination of supercooled droplets using Laser-Induced Fluorescence', *Exp. Fluids*, 2019.

[9]   H. Strausky, J. R. Krenn, A. Leitner, and F. R. Aussenegg, 'Thickness determination of a water film on dye-doped ice by fluorescence spectroscopy', *Appl. Opt.*, vol. 35, no. 1, p. 198, Jan. 1996.

[10] W. Chaze, O. Caballina, G. Castanet, and F. Lemoine, 'The saturation of the fluorescence and its consequences for laser-induced fluorescence thermometry in liquid flows', *Exp. Fluids*, vol. 57, no. 4, Apr. 2016.

[11] S. E. Wood, M. B. Baker, and B. D. Swanson, 'Instrument for studies of homogeneous and heterogeneous ice nucleation in free-falling supercooled water droplets', *Rev. Sci. Instrum.*, vol. 73, no. 11, pp. 3988–3996, Nov. 2002.

[12] B. Abramzon and W. Sirignano, 'Droplet vaporization model for spray combustion calculations', *Int J Heat Mass Transf.*, vol. 32, no. 9, pp. 1605–1618, 1989.